PROCEEDINGS OF SPIE

SPIEDigitalLibrary.org/conference-proceedings-of-spie

Photoinduced optical dynamics of phase-change vanadium oxides

Nardeep Kumar
Armando Rúa
Lee R. Chevres
Larry Theran
Brian Ayala
Félix E. Fernández
Sergiy I. Lysenko

SPIE.

Photoinduced optical dynamics of phase–change vanadium oxides

Nardeep Kumar, Armando Rúa, Lee R. Chevres, Larry Theran, Brian Ayala, Félix E. Fernández, Sergiy Lysenko[1*]

Department of Physics, University of Puerto Rico, Mayaguez, Puerto Rico 00681, USA

ABSTRACT

Using time- and angle-resolved hemispherical elastic light scattering technique we reveal complex pathways of photoinduced nonlinear optical dynamics in VO_2, V_2O_3 and V_3O_5 thin films. The structural dynamics was monitored by using an ultrafast diffraction conoscopy technique. The evolution of phases in these correlated oxides is substantially different and significantly depends on optical excitation, temperature and size of grains and domains. Strong optical nonlinearity along with its complex transient dynamics makes vanadium oxides attractive for high-contrast all-optical switches, high-speed optical data storage and holographic devices. The characteristic time of optical nonlinearity can be tuned from several femtoseconds to picoseconds by altering the excitation fluence and size of grains and domains. Additional control of ultrafast phase transition dynamics can be achieved by photoacoustical generation of strain waves. Depending on material morphology and level of optical excitation, the optical signal shows coherent oscillations caused by photoacoustic wave at picosecond and nanosecond time scales. Complex nonlinear dynamics of correlated vanadium oxides can provide a way for precise tuning of transient optical and electronic properties in photonic devices.

Keywords: elastic light scattering, ultrafast diffraction conoscopy, correlated vanadium oxides

1. INTRODUCTION

Vanadium is a *d*-transition metal and a variety of stoichiometric oxides of vanadium exist in both single as well as mixed valence states. Most of the vanadium oxides can be categorized into Magnéli (V_nO_{2n-1})[1] or Wadsley ($V_{2n}O_{5n-2}$)[2] homologous series. They belong to an important class of materials with exotic physical and chemical properties[3], but it is the metal-insulator transition (MIT)[4] which has attracted major attention. The oxides exhibit MIT at different temperatures T_c: T_c=150 K (V_2O_3)[3], T_c=340 K (VO_2)[3] and, although much less studied so far, V_3O_5 with T_c= 428 K[5].

In this article, we report on ultrafast nonlinear optical (NLO) dynamics of VO_2, V_2O_3 and V_3O_5. The method of ultrafast diffraction conoscopy (UDC)[6] was applied to monitor the photoinduced structural phase transition (SPT) in VO_2 and NLO response of V_2O_3. By monitoring the evolution of conoscopy patterns for VO_2, we demonstrate the lattice distortion during the photoinduced phase transition process. At the same time, by exploring the transient polarization of scattered light the presence of a transient intermediate state with biaxial symmetry is revealed. However, for the case of V_2O_3, by monitoring the conoscopy patterns of scattered light we observe strong optical nonlinearity but without any noticeable change in the lattice symmetry.

Finally, we use results from hemispherical elastic light scattering to study optical nonlinearity in V_3O_5 thin films. Our study shows noticeable anisotropic grain size dependence of thermal phase transition and ultrafast optical nonlinearity, revealing significant differences between thermal and light induced dynamics.

sergiy.lysenko@upr.edu

Active Photonic Platforms IX, edited by Ganapathi S. Subramania, Stavroula Foteinopoulou, Proc. of SPIE Vol. 10345, 103451F · © 2017 SPIE · CCC code: 0277-786X/17/$18 · doi: 10.1117/12.2274092

2. EXPERIMENTAL METHODS

2.1 Sample preparation

Pulsed laser deposition (PLD) technique was used to prepare a thin film of VO_2/Al_2O_3 (A-cut) with 80 nm thickness. Thin films of V_2O_3/Al_2O_3-R-cut (120 nm) and V_3O_5/SiO_2 (120 nm) were grown by using reactive DC magnetron sputtering from a vanadium (99.95% purity) target. Table 1 shows the growth conditions for these three samples.

Table 1. Growth conditions for VO_2, V_2O_3 and V_3O_5 films.

Process	Sample	Chamber pressure (mTorr)	Energy	Gas flow (sccm)	Substrate temperature (^oC)
PLD	VO_2	50	Fluence = 4 (J/cm^2)	Argon = 10, Oxygen = 15	550
DC magnetron sputtering	V_2O_3	21	Power = 300 W	Argon = 35, Oxygen = 2.6	500
	V_3O_5	21	Power = 300 W	Argon = 35, Oxygen = 2.6	475

2.2 Experimental technique

Angle-resolved elastic light scattering and ultrafast diffraction conoscopy measurements were performed with a scatterometer setup which has been described elsewhere[6]. The Spectra Physics Ti:Sapphire laser system was employed for pump-probe optical measurements. The regeneratively amplified laser pulses with central wavelength λ = 800 nm were compressed to 130 femtosecond duration. Output radiation was split by a beam splitter into a pump and a probe. The probe pulse was frequency doubled by 100 μm thick beta barium borate (BBO) crystal. A pump-probe wavelength combination (λ=800 and λ=400 nm, respectively) was used to collect NLO signal from VO_2, V_2O_3 and V_3O_5 thin films. Circularly polarized pump and vertically polarized probe pulses were normally focused to spot sizes of 0.6 mm and 70 μm diameters respectively. The timing between pump and probe pulses was controlled by electromechanical optical delay line. The scattering signal was recorded and mapped for both polar θ and azimuthal φ angles, using a Bidirectional-Scatter-Distribution-Function (BSDF) which is defined as follows[7]:

$$BSDF(\theta,\varphi) = \frac{1}{I_0}\left(\frac{dI_S(\theta,\varphi)}{d\Omega}\right)\frac{1}{cos\theta} \quad (1),$$

where I_0 is the incident light intensity, and dI_S is the scattered light intensity measured within a solid angle $d\Omega$.

3. RESULTS AND DISCUSSION

3.1 VO_2

Out of all the known oxides of vanadium only two oxides VO_2 and V_3O_5 show phase transitions above room temperature[3,5]. VO_2 has complex phase transition process which involves electron-electron correlation and electron-lattice interactions[4, 8-11]. One approach to study its complex phase transition processes is to track electronic and structural transition dynamics separately.

For the work presented here we used ultrafast diffraction conoscopy (UDC) technique to study the VO_2 phase transition by monitoring only the transient change of lattice symmetry. This technique allows us to study the transformation of lattice symmetry during the phase transition process. With the help of UDC, we directly monitor not only changes in the sample's surface inhomogeneities[12-15], but also track the biaxial to uniaxial symmetry change, revealing an intermediate transient state[6].

The photoexcitation of VO_2 can produce a photoinduced[9] insulator-to-metal phase transition (IM PT), a non-thermal process, which is different from the thermally driven[3] IM PT. Measured BSDF indicatrices for 80-nm-thick VO_2/Al_2O_3

(A-cut) film for various probe delays are shown in Figure 1(a), upper panel. The scans were performed at a pump energy fluence of F = 8 mJ/cm^2.

At zero probe delay the scattering signal shows two hyperbolas associated with biaxial isogyres [see supplementary information in Ref. 6], in opposite quadrants. During the phase transition interval, the separation between these two hyperbolas starts to decrease and disappears after 500 fs. After the phase transition, the two hyperbolas merge to form a cross-like pattern associated with uniaxial isogyres. The evolution from biaxial to uniaxial symmetry is consistent with the transformation from monoclinic VO_2 to rutile VO_2.

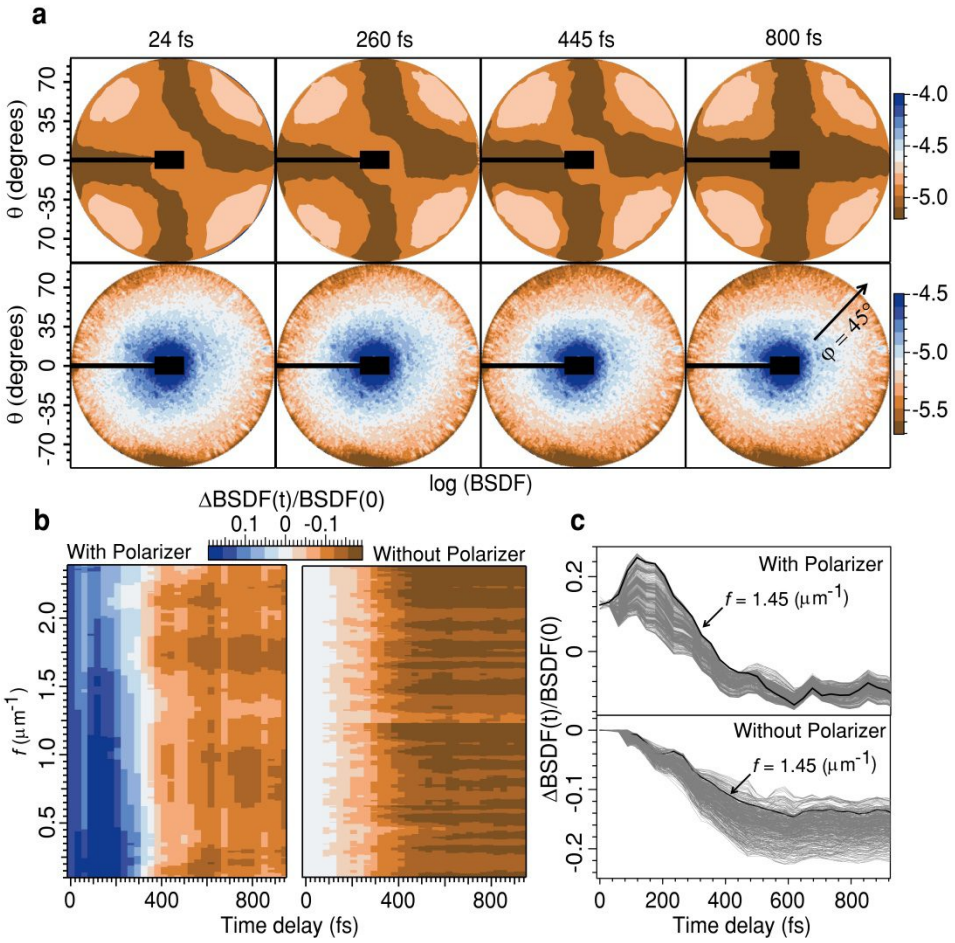

Figure 1. (a) Evolution of light scattering indicatrix with (upper panel) and without (lower panel) the analyzer. (b) Cross-section map of transient light scattering with (left panel) and without (right panel) the analyzer for different spatial frequencies *f* at an azimuthal angle φ = 45°. (c) Transient light scattering plot from the cross-section map with (upper panel) and without (lower panel) the analyzer.

Figure 1(b) shows time-dependent cross-sections of the scattering indicatrices with (left panel) and without (right panel) the analyzer mapped at azimuthal direction φ = 45° versus spatial frequency. With the analyzer, the transient scattering signal at different spatial frequencies shows a strong rise, which peaks around 180 fs, before attaining a constant minimum level after 400 fs. This rise of UDC signal reveals the formation of an intermediate transient state of VO_2 during the SPT.[6]

To show the significance of UDC technique, we compare the UDC results with ultrafast light scattering data obtained without analyzer. The lower panel of Figure 1(a) shows the BSDF (θ, φ) indicatrices for various probe delays collected by removing the analyzer from the setup. As compared to UDC results, the scattering evolution without analyzer shows a

continuous decrease of the signal without any noticeable intermediate increase of scattering signal during the phase transition interval.

To further clarify the SPT, we plot in Figure 1(c) the cross-section of the data mapped in Figure 1(b) for all the spatial frequencies from $f = 0.5\ \mu m^{-1}$ to $f = 2.4\ \mu m^{-1}$ with (upper panel) and without (lower panel) the analyzer. From these cross-sections, we see that the rise of the scattering signal depends upon the spatial frequency. For small spatial frequencies, the rise (upper panel) is more pronounced than for higher spatial frequencies.

Spatial frequency dependent scattering signal is an important result because spatial frequency f is related to the characteristic size d of mesoscale irregularities within the film. The relation between them is defined as $f=1/d=\sin\theta/\lambda$.[7, 16, 17] The spatial frequency interval from $f = 0.5\ \mu m^{-1}$ to $f = 2.4\ \mu m^{-1}$ corresponds to microstructures of the VO_2 film with characteristic sizes from $d = 2.0\ \mu m$ to $d = 0.42\ \mu m$, respectively. The results obtained indicates that the smaller microstructures contribute less in depolarization of scattering signal during structural phase transition, as compared to large size microstructures.

3.2 V_2O_3

In the past several decades the thermal phase transition of V_2O_3, which occurs at T_c~150 K, has been intensively studied and by now it is well known that this structural transition, in which the corundum-type V_2O_3 lattice transforms to a monoclinic lattice structure, is accompanied by a metal-insulator transition from a paramagnetic metal phase to an antiferromagnetic insulator phase.

In recent studies, it has been shown that the photoexcitation can also change the electronic properties of V_2O_3[18-20]. However, very little is known about structural transitions of V_2O_3 during photoexcitations beyond the PT temperature. One way to study SPT dynamics of V_2O_3 upon photoexcitation is by collecting data related only to the structural properties. By employing the UDC technique, we can just focus on properties of V_2O_3 related to structural dynamics. For this study, we kept the sample at room temperature, which is well above the T_c point. Hence, the collected nonlinear signal is solely due to the photoexcitation.

Figure 2(a) shows the time-resolved ultrafast diffraction conoscopy indicatrices at various time scales from 0 ps to 100 ps. There is a clear change in the scattering signal for different polar angles when time changes from 0 ps to 100 ps, indicating a strong photoinduced nonlinear response. With the help of UDC technique we can answer whether this photoinduced nonlinear change is related to the structural change or not. Evolution of log (BSDF) indicatrices show that, compared to VO_2 [Fig. 1(a)], the V_2O_3 results [Fig. 2(a)] do not indicate any change in the symmetry of the crystal on the timescale from 0 ps to 100 ps. This is an important result indicating that the strong photoinduced scattering response we see is not related to the structural phase transition. Further studies are needed to explore the mechanism behind the photoinduced nonlinear response of V_2O_3 at room temperature.

To explore the characteristic size dependence of the nonlinearity, we map the cross sections of scattering patterns [Fig. 2(b)] for different spatial frequencies at an azimuthal angle $\varphi = 45°$, as a function of time delay. Compared to VO_2, the scattering cross-section map of V_2O_3 shows more pronounced variation with spatial frequencies. Within ~25 ps, the nonlinearity is quite uniform for all the spatial frequencies. However, strong variation of scattering signal starts to appear after ~25 ps; above $f \sim 1.1\ \mu m^{-1}$, the nonlinearity is stronger than for lower spatial frequencies. If the observed photoinduced scattering signal is related to the PT dynamics, then this non-uniformity of scattering nonlinearity indicates that for small structures, $d < 0.9\ \mu m$ ($f > 1.1\ \mu m^{-1}$), the MIT process takes a longer time than for structures with $d > 0.9\ \mu m$. This could be due to size-dependent variations in the internal strain of the film microstructures.

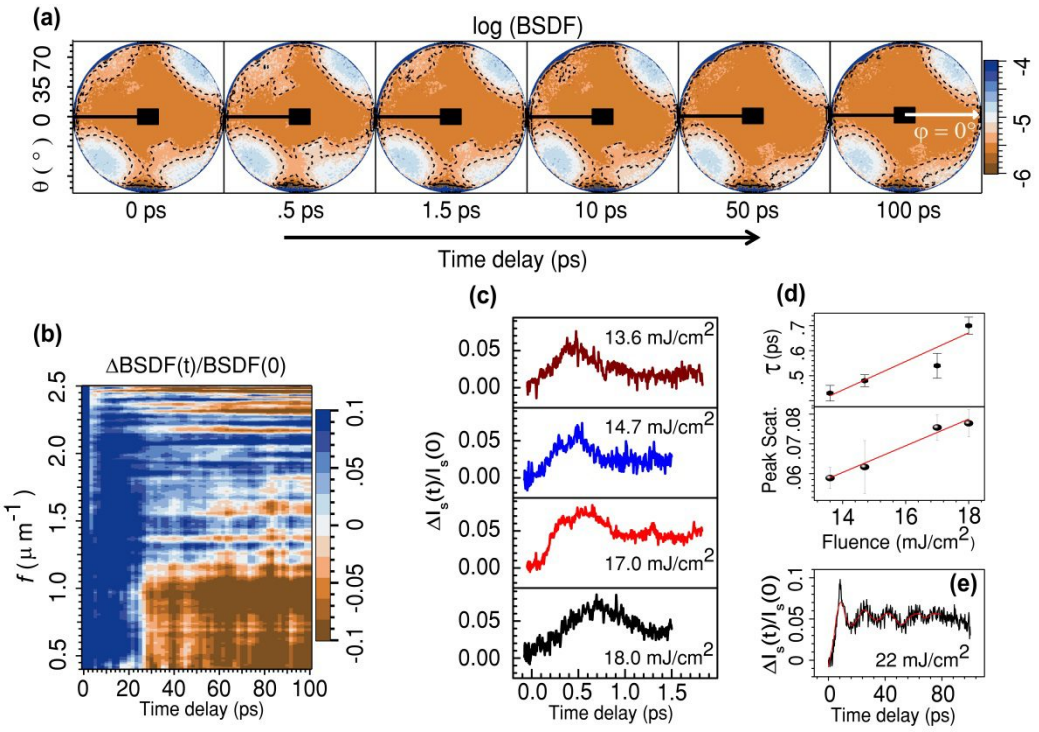

Figure 2. (a) Evolution of the transient ultrafast conoscopy log (BSDF). (b) Cross-section map of transient light scattering for different spatial frequencies (f) at an azimuthal angle φ = 45°. (c) Transient light scattering $\Delta I_s(t)/I_s(0)$, where $\Delta I_s(t)=I_s(t)-I_s(0)$, versus probe delay at different pump fluences without the analyzer. (d) Upper panel; characteristics rise time of $\Delta I_s(t)/I_s(0)$ signal for reaching the peak measured at each fluence, lower panel; maximum value of $\Delta I_s(t)/I_s(0)$ signal measured at each fluence level. Solid lines are linear fits. (e) Differential scattering signal at F = 22 mJ/cm^2. Solid line indicates a sinusoidal fit of oscillatory signal component.

Figure 2(c) shows the transient light scattering $\Delta I_s(t)/I_s(0)$ collected within 2 ps at different fluence levels. The rise time τ and peak scattering (Peak Scat.) of the transient scattering signal show a linear dependence with fluence, as shown in Figure 2(d) and 2(e). With increasing fluence, the transient signal starts to show an oscillating behavior. Fitting $\Delta I_s(t)/I_s(0)$ with a sinusoidal function gives a period of 18 ps. The oscillatory response of V_2O_3 at relatively high pump fluence is very different from NLO response of VO_2, which shows coherent oscillations at low fluence levels[21, 22].

3.3 V_3O_5

V_3O_5 which is the first member of Magnéli phases undergoes an insulator-to-metal phase transition at temperature T_c~428 K[5, 23, 24]. While the thermal phase transition of V_3O_5 has been well known[5], information related to the photoexcited nonlinear dynamics has only recently been explored[25]. Here, we use ultrafast hemispherical angle-resolved light scattering technique to monitor the thermally driven IM-PT process and photoinduced nonlinear response of a 120 nm thick V_3O_5/SiO_2 film.

First, we performed stationary scattering measurements using a continuous wave laser of wavelength 450 nm to study the thermally induced PT process. The sample was mounted on a heater for controlling the temperature. In order to study the PT process from the illuminated surface area of the film, the scattered light was collected over a hemisphere and mapped by BSDF (θ,φ), as shown in Figure 3(a). The BSDF indicatrix allows visualizing the optical response of individual group of microstructures with different azimuthal orientations and spatial frequencies. The log (BSDF) scattering patterns reveal new information about multi-scale PT dynamics. Starting from the insulating phase at room temperature (300 K),

scattering intensity continuously drops at all spatial frequencies through the IM PT. Initially, all spatial frequencies show a uniform scattering signal. However, some spatial frequency dependent scattering anisotropy starts to appear after 300 K and becomes clearly visible at ~430 K, as can be seen from changes in the indicatrix, as shown in Figure 3(a).

Figure 3(b) shows the sample resistivity ρ as a function of temperature, measured using a 4-point van der Pauw configuration. From the resistivity curve, one can see that the I-M PT occurs at T_c~430 K.

Strong NLO response of V_3O_5 was observed upon photoexcitation of the film. Figure 3(c) shows the transient light scattering $\Delta I_s(t)/I_s(0)$ measured at different temperatures with a pump Fluence F = 14 mJ/cm^2. At each temperature, the transient scattering signal shows a rapid drop within 900 fs, which is then followed by a slow decrease lasting upto several picoseconds.

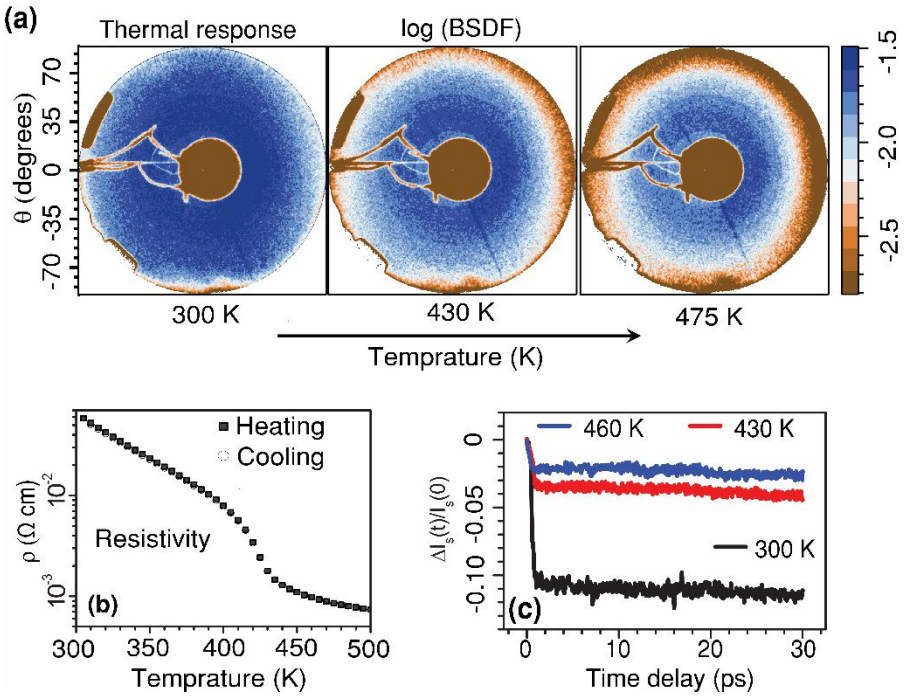

Figure 3. (a) Evolution of light scattering indicatrices during thermally induced insulator-to-metal phase transition. (b) Change of the resistivity ρ as a function of sample temperature. (c) Transient light scattering $\Delta I_s(t)/I_s(0)$, where $\Delta I_s(t)=I_s(t)-I_s(0)$, versus probe delay at different sample temperatures.

To obtain additional information about the ultrafast optical response of individual microstructures, we measured the transient scattering signal BSDF(θ, φ) at room temperature. BSDF indicatrices for various probe delays are shown in Figure 4(a). Compared to scattering indicatrices obtained versus temperature, the transient indicatrices show a higher order of anisotropy. For this V_3O_5 film the penetration depth for pump and probe were measured to be 30 nm and 25 nm respectively. Lower penetration depth of the probe as compared to the pump pulse allows us to monitor the nonlinear dynamics for a uniformly excited sample within the probe's penetration depth.

Each scattering indicatrix shows a rhombus type pattern, as denoted by dashed lines in the figure. This is a surprising result, as V_3O_5 on a SiO_2 substrate should not have any preferred in-plane orientation of crystallites. This shows an advantage of hemispherical angle-resolved light scattering technique, which can easily detect even a small anisotropy in the film. With increasing probe delay the scattering intensity rapidly drops and the size of the rhombus type pattern decreases from $0°<\theta<65°$ at t = 0 fs to $0°<\theta<40°$ at t = 900 fs.

To investigate the ultrafast nonlinear scattering response with characteristic size, we map the cross-sections of scattering patterns with various spatial frequencies (*f*) at an azimuthal angle φ = 45° as a function of time delay [Fig. 4(b)]. As seen from the map, the scattering response of V_3O_5 is more or less uniform for all spatial frequencies.

Figure 4(c) shows the transient light scattering $\Delta I_s(t)/I_s(0)$, for nanosecond time delay range, measured at different pump fluences. At each fluence level, the scattering signal first shows a rapid drop within few picoseconds followed by a relatively slow component lasting upto several nanoseconds. As shown previously[25], the total integrated scattering signal of V_3O_5 rapidly drops within 800 fs. Similar dynamics has been detected for photoexcited VO_2 where rapid drop of scattering signal takes place within ~500 fs, indicating a photoinduced IM PT[6]. The ultrafast nonlinear optical response of V_3O_5 is associated with photoinduced phase transition[26]. However, further exploration is required to find the pathways of photoexcited dynamics of V_3O_5.

From the fluence–dependent transient scattering data [Fig. 4(c)] one can see that the pronounced oscillations, with a period of 120 ps, start to appear at high fluence F ~ 24 mJ/cm^2. This reflects some similarity between V_3O_5 and V_2O_3, in which acoustical phonons start to appear only at high fluence[26].

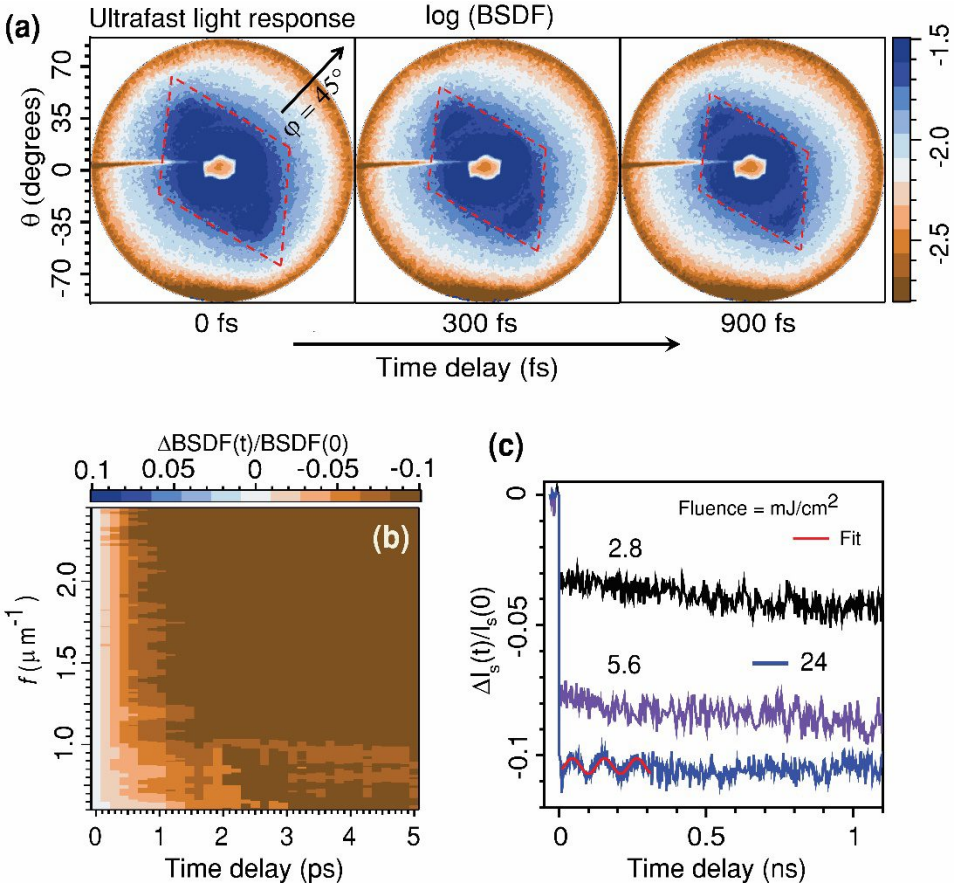

Figure 4. (a) Evolution of light scattering indicatrices with light excitations. (b) Cross-section map of transient light scattering for different spatial frequencies (*f*) at an azimuthal angle φ = 45°. (c) Transient light scattering $\Delta I_s(t)/I_s(0)$, where $\Delta I_s(t)=I_s(t)-I_s(0)$, versus probe delay at different pump fluences.

4. CONCLUSIONS

In conclusion, we have investigated the time-resolved hemispherical light scattering from VO_2, V_2O_3 and V_3O_5 vanadium oxide thin films. Our results show some similarities and differences between photoinduced dynamics of these three vanadium oxides. We have tracked the structural phase transition dynamics of VO_2 and V_2O_3 using ultrafast diffraction conoscopy. Obtained results show that in the case of VO_2 there is a strong structural phase transition accompanied by a transient biaxial intermediate state. On the other hand, no noticeable variation in the conoscopy patterns has been detected from V_2O_3, indicating no structural phase transition. Photoexcited transient scattering, on sub-picosecond time scale, from VO_2 and V_3O_5 show a rapid decrease while it increases for V_2O_3. NLO response of these oxides is associated with phase transition processes. A pronounced characteristic size-dependence in scattering response was resolved for VO_2 and V_2O_3 films. Our results also reveal strong oscillatory behavior of the ultrafast scattering signal for V_2O_3 and V_3O_5 when the pump fluence approaches a relatively high value, contrary to VO_2 which can show oscillatory behavior due to acoustical and optical phonons only in low fluence regime.

We have presented many interesting results related to photoinduced nonlinear dynamics in VO_2, V_2O_3 and V_3O_5. However, much more work on single crystals and/or highly oriented epitaxial films is required to determine the relationship between photoinduced nonlinearity and the phase transition processes. We expect that the experimental results reported here set the stage for more in-depth theoretical and experimental analysis of the photoinduced solid-to-solid phase transitions and nonlinear optical dynamics of phase-change vanadium oxides.

ACKNOWLEDGEMENTS

This work is sponsored by the U.S. Army Research Laboratory and the U.S. Army Research Office under contract number W911NF-15-1-0448.

REFERENCES

[1] Schwingenschlögl U. and Eyert V., "The vanadium Magnéli phases V_nO_{2n-1}," Ann. Phys. 13(9), 475–510 (2004).

[2] Wadsley, A.D., "Nonstoichiometric Metal Oxides. Order and Disorder," Nonstoichiometric Compounds 39, 23–36 (1963).

[3] Morin, F. J., "Oxides which show a metal-to-insulator transition at the neel temperature," Phys. Rev. Lett. 3(1), 34–36 (1959).

[4] Imada, M., Fujimori, A. and Tokura, Y., "Metal-insulator transitions," Rev. Mod. Phys. 70(4), 1039 (1998).

[5] Landolt-Bornstein: Numerical Data and Functional Relationships in Science and Technology - New Series - Group III Condensed Matter, edited by H. P. J. Wijn, Vol. 27G, Springer-Verlag, (1992).

[6] Kumar, N., Rúa, A., Fernandez, F. E. and Lysenko, S., "Ultrafast diffraction conoscopy of the structural phase transition in VO_2: Evidence of two lattice distortions," Phys. Rev. B 95(23), 235157 (2017).

[7] Stover, J. C., [Optical Scattering Measurement and Analysis], SPIE Optical Engineering Press, Bellingham; Washington USA, (1995).

[8] Goodenough, J. B., "The two components of the crystallographic transition in VO_2," J. Solid State Chem. 3(4), 490 500 (1971).

[9] Cavalleri, A., Dekorsy, T., Chong, H. H. W., Kieffer, J. C. and Schoenlein, R. W., "Evidence for a structurally-driven insulator-to-metal transition in VO_2: a view from the ultrafast timescale," Phys. Rev. B 70(16), 161102 (2004).

[10] Dagotto, E., "Complexity in strongly correlated electronic systems," Science 309(5732), 257–262 (2005).

[11] Lee, P. A., Nagaosa, N. and Wen, X. G., "Doping a Mott insulator: Physics of high-temperature superconductivity," Rev. Mod. Phys. 78(1), 17-85 (2006).

[12] Zerrad, M., Lequime, M. and Amra, C., "Spatially resolved surface topography retrieved from far-field intensity scattering measurements," Appl. Opt. 53(4), A297–304 (2014).

[13] Herffurth, T., Schröder, S., Trost, M., Duparré, A. and Tünnermann," A. Comprehensive nanostructure and defect analysis using a simple 3D light-scatter sensor," Appl. Opt. 52(14), 3279–3287 (2013).

[14] Harvey, J. E., Schröder, S., Choi, N. and Duparré, A., "Total integrated scatter from surfaces with arbitrary roughness, correlation widths, and incident angles," Opt. Eng. 51(1), 13402 (2012).

[15] Sorrentini, J., Zerrad, M. and Amra, C., "Statistical signatures of random media and their correlation to polarization properties," Opt. Lett. 34(16), 2429–2431 (2009).

[16] Elson, J., Rahn, J. and Bennett, J., "Relationship of the total integrated scattering from multilayer-coated optics to angle of incidence, polarization, correlation length, and roughness cross-correlation properties," Appl. Opt. 22(20), 3207-3219 (1983).

[17] Schröder, S., Duparre, A., Coriand, L., Tünnermann, A., Penalver, D. and Harvey, J., "Modeling of light scattering in different regimes of surface roughness," Opt. Express 19(10), 9820-9835 (2011).

[18] Kumar, N., Rúa, A., Díaz, R., Castillo, I., Ayala, B., Cita, S., Fernández, F. and Lysenko, s., " Time-resolved light scattering by photoexcited V_2O_3," MRS Adv. 23 (2), 1231-1236 (2017).

[19] Abreu, E., Wang, S., Ramírez, J. G. , Liu, M. , Zhang, J., Geng, K., Schuller, I. K. and Averitt, R. D., "Topological nodal line semimetals with and without spin-orbital couplingness," Phys. Rev. B 92(8), 085130(R) (2015).

[20] Liu, M. K., Pardo, B., Zhang, J. , Qazilbash, M. M. , Yun, S. J., Fei, Z., Shin, J. H., Kim, H. T., Basov, D. N. and Averitt, R. D., "Photoinduced Phase Transitions by Time-Resolved Far-Infrared Spectroscopy in V_2O_3," Phys. Rev. Lett. 107(6), 066403 (2011).

[21] O'Callahan, B. T., Jones, A. C., Hyung Park, J., Cobden, D. H., Atkin, J. M. and Raschke, M. B., "Inhomogeneity of the ultrafast insulator-to-metal transition dynamics of VO_2," Nat. Commun. 6, 6849 (2015).

[22] Abreu, E., Corder, S. N. G., Yun, S. J., Wang, S., Ramirez, J. G., West, K., Zhang, J., Kittiwatanakul, S., Schuller, I. K., Lu, J., Wolf, S. A., Kim, H.-T. , Liu, M. and Averitt, R. D., "Ultrafast Electron-Lattice Coupling Dynamics in VO_2 and V_2O_3 Thin Films," arXiv:1701.05531 (2017).

[23] Åsbrink, S. and Hong, S.H., "Increase of X-ray reflection intensities and profile widths at the low- to high-V_3O_5 phase transition state," Nature 279, 624−625(1979).

[24] Chudnovslii, F. A., Terukov, E. I. and Khomskii, D. I., "Insulator-metal transition in V_3O_5," Solid State Commun. 25(8), 573−577(1978).

[25] Rúa, A., Díaz, R. D., Kumar, N., Lysenko, S. and Fernández, F., "Metal-insulator transition and nonlinear optical responseof sputter-deposited V_3O_5 thin films ," J. Appl. Phys. 121(23) 235302 (2017).

[26] Kumar, N., Rúa, A., Lu, J., Fernandez, F. E. and Lysenko, S., "Ultrafast excited-state dynamics of V_3O_5 as a signature of a photoinduced insulator-metal phase transition," Phys. Rev. Lett. Accepted (2017).